

An advanced theory of the strength of hybrid composites

HIROSHI FUKUDA

Institute of Interdisciplinary Research, University of Tokyo, 4-6-1 Komaba, Meguro-ku, Tokyo 153, Japan

This paper proposes a statistical approach to the strength of a unidirectionally-arrayed hybrid sheet. This paper proposes of modification of the theory proposed by Zweben. The concept of the hybrid effect has been clarified and the present theory has been compared with experimental data. Quantitative evaluation of the hybrid effect and stress-strain behaviour of hybrids is possible, although there remain some discrepancies between experimental data and theoretical prediction. Stress (or strain) concentration factors and ineffective length around a discontinuous fibre are calculated in a more precise manner, which are used for a statistical approach.

Nomenclature

A	cross-sectional area of a fibre
d	distance of fibres
E	Young's modulus of a fibre
G	shear modulus of matrix
h	thickness of sheet
HE	high elongation fibre
k	stress concentration factor
L	length of specimen
LE	low elongation fibre
M_h	number of links of each fibre
N	total number of fibres
P_h	probability of break of one adjacent LE fibre
P_{2h}	probability of break of at least one of two adjacent LE fibres
p, q, r, s	Weibull parameters
R	ratio of extensional rigidities of two fibres
R_ϵ	hybrid effect
u_m	displacement of m -th fibre
V_m	influence function
X_{1h}	expected number of scattered fibre breaks
X_{2h}	expected number of the break of nearest LE fibres
δ_h	ineffective length
ϵ_{2h}	composite failure strain
h (subscript)	hybrid
m (subscript)	m -th fibre
* (superscript)	value for HE fibre

1. Introduction

Composite materials containing two or more types of fibres in a common matrix have become well known as hybrid composites. A graphite fibre-reinforced composite is an attractive material because of its high strength- and stiffness-to-density ratios and it is much used in the aerospace field where light weight structures are required. On the other hand, this material has the disadvantage that the ultimate failure strain is small. To compensate for this defect, a hybrid composite has been designed. A Kevlar[®]/graphite hybrid, for example, has been selected as the material for the Boeing 767 aircraft [1]. In 1972 many papers on hybrid composites were reported [2-6]. It is interesting to note that a concept of hybridization was born shortly after graphite fibre composites began to be used. A state-of-the-art review of hybrid composites can be found in the papers by Chou and Kelly [7], Renton [8], and Fukuda [9].

According to Manders and Bader [10, 11], there are two ways of understanding the failure of a composite, that is, fracture mechanical (thermodynamic) and micromechanical (statistical) approaches. The present paper belongs to the latter category.

Many statistical works on the strength of non-hybrid composites has been reported hitherto

[12–27] and these approaches are now applied to hybrid composites [28–31].

Zweben [28] was the first to deal with the strength of hybrid composites from a statistical view point, the idea of which may be called a “diplet” of Batdorf’s terminology [25, 26]. But his paper has unclear points which are discussed further.

First, as was described in the Introduction of his paper, he intended to make clear the phenomenon of a “hybrid effect.” The term hybrid effect implies that the initial failure strain of a hybrid composite (which corresponds to the failure of low elongation fibres in a hybrid) is greater than failure strain of a low-elongation, non-hybrid composite. However, in Zweben’s analysis, the failure of a HE fibre adjacent to a broken LE fibre is discussed. Therefore, his paper seems a little far from the explanation of the hybrid effect.

Next, he says his theory is a lower bound on composite failure strain. He focused on the failure of a HE fibre adjacent to one discontinuous LE fibre. In the case of a non-hybrid composite, this approach will lead to a lower bound, as has been discussed in [13]. This may not be true in a hybrid composite for the reason that when one LE fibre is broken, next failure is expected not on the adjacent HE fibre but on the adjacent LE fibre because the failure strain of HE fibres is much larger than that of LE fibres. Thus one HE fibre can be surrounded by two discontinuous LE fibres. In this case the stress (or strain) concentration factor (SCF) of the HE fibre becomes larger than k_h [28].

Lastly, the ineffective length and the SCF calculated by Zweben are not accurate because he used too small a model. In a non-hybrid composite, his approximate model [32] predicts smaller SCFs than those of Hedgepeth’s shear-lag analysis of an infinite medium [33]. This discrepancy will occur in the hybrid composite also. The smaller SCF predicts a larger composite strength; this could be dangerous.

These points are modified in this paper, although the primary idea is credited to Zweben.

2. Analysis

There are two kinds of unidirectional hybrid composites, that is, an interply (interlaminated) hybrid and an intraply (intermingled) hybrid (cf. Fig. 1). We consider here an intraply hybrid sheet (Fig. 1b) in which two kinds of fibres assume alternating

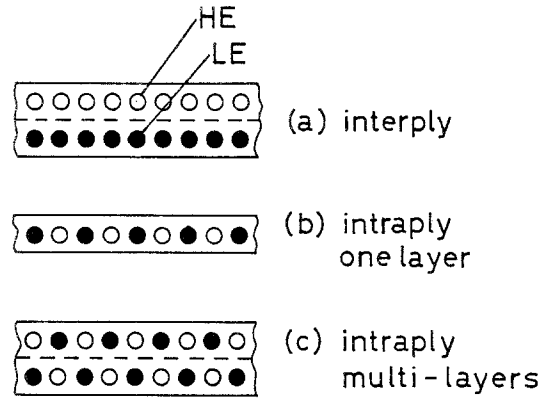


Figure 1 Cross-sectional view of hybrid composites.

positions with equal distance, d . A bundle of fibres (impregnated yarn) can be considered as if it were an individual fibre [28]. The analytical model considered here is shown in Fig. 2, where one LE fibre is discontinuous. A tensile load is applied in the fibre direction. The axial length of the specimen is L and δ_h is so called an ineffective length [12]. Thus each fibre consists of $M_h = L/\delta_h$ links. The total fibres in the composite is N , of which $N/2$ are LE, and $N/2$ are HE fibres.

We assume here that the cumulative distribution functions for the failure strains of the LE and HE fibres of the length l are given, respectively, by a Weibull distribution of the form

$$F(\epsilon) = 1 - \exp(-ple^q) \quad (1)$$

$$F^*(\epsilon) = 1 - \exp(-rle^s)$$

where, p , q , r and s are Weibull parameters and an asterisk (*) is used for defining quantities related to HE fibres.

Consider, for example, a hybrid composite of a graphite/glass combination. The ultimate failure strain of a graphite fibre (LE fibre) is approximately one third of that of a glass fibre (HE fibre). Then it is natural to consider that an LE fibre will break first. When the composite is subjected to a strain ϵ , the expected number of scattered fibre

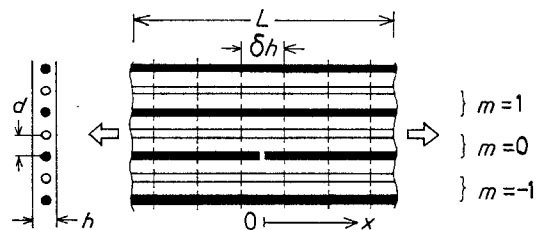


Figure 2 Model of analysis.

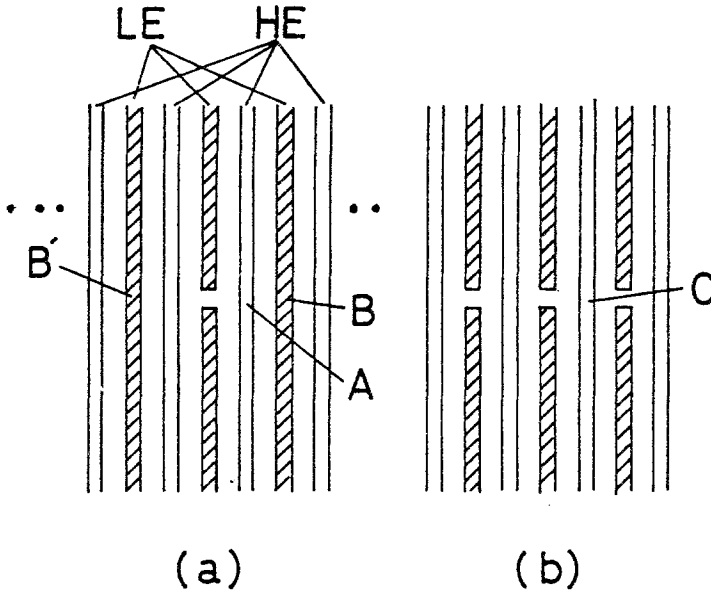


Figure 3 Failure of fibre(s): (a) a model of only one broken fibre; (b) a model of all LE fibres being broken.

breaks in the $N/2$ LE fibres is

$$X_{1h} = \frac{1}{2} M_{hr} N F(\epsilon) \quad (2)$$

We will now discuss what happens next after one LE fibre is broken. When an LE fibre is broken, stress (or strain) concentration will occur to continuous fibres adjacent to the broken fibre. Suppose the SCFs of fibres A and B of Fig. 3a are k_h^* and k_h , respectively. These values are derived in the Appendix. Although k_h is smaller than k_h^* , the fibre B will possibly break prior to the failure of A because the ultimate failure strain of LE fibres is smaller than that of HE fibres.

We will consider first the probability of the nearest LE fibre (fibre B) being broken. The probability that fibre B will break under the strain concentration k_h is

$$P_h = \frac{F(k_h \epsilon) - F(\epsilon)}{1 - F(\epsilon)} \quad (3)$$

The explanation of the denominator is briefly shown in [14] and [34].

The model considered is symmetric. Therefore, the probability of failure of the fibre B' of Fig. 3a is the same as Equation 3. Thus the probability that at least one of the two overstressed LE fibres will break is

$$P_{2h} = 1 - (1 - P_h)^2 \quad (4)$$

The expected number of sites where a scattered LE fibre break is followed by the fracture of at least one of the nearest overstressed LE fibres is

$$X_{2h} = X_{1h} P_{2h} \quad (5)$$

If we define a failure of composites as the fracture of one of the nearest LE fibres, this event is expressed as:

$$X_{2h}(\epsilon_{2h}) = 1 \quad (6)$$

where ϵ_{2h} is the composite strain at which the nearest LE fibre will break. We pay attention here to the failure of the nearest LE fibre and hence this may be called a di-plet [25, 26]. But there exists a continuous HE fibre between two LE fibres of interest. Thus our model is a little different from the di-plet.

Although we can solve Equation 6 directly by substituting Equations 1 to 5, the following assumptions are introduced [28] in order to get a good prospect:

$$1 - F(\epsilon) \approx 1 \quad \text{in Equation 3}$$

$$P_{2h} \approx 2P_h \quad \text{in Equation 4}$$

$$\exp(-ple^q) \approx 1 - ple^q \quad \text{in Equation 1}$$

(7)

Thus the failure strain is calculated as

$$\epsilon_{2h} = [NL\delta_{hr} p^2 (k_h^q - 1)]^{-1/2q} \quad (8)$$

Next we will discuss the failure strain of fibre A of Fig. 3a being broken. In this case, Equation 3 should be changed to

$$P_h^* = \frac{F^*(k_h^* \epsilon) - F^*(\epsilon)}{1 - F^*(\epsilon)} \quad (9)$$

and the final result is

$$\epsilon_{2h}^* = [NL\delta_{hr} p r (k_h^{*s} - 1)]^{-1/(q+s)} \quad (10)$$

This is the same as Equation A10 of Zweben's paper [28], except for the notation.

As was described before, the LE fibres are easy to break. Therefore, it is possible that all LE fibres break prior to the failure of the HE fibres (cf. Fig. 3b). In this case, the SCF of the HE fibre (fibre C of Fig. 3b) becomes

$$k_h^* = 1 + EA/E^*A^* \quad (11)$$

Equation 11 just indicates that the applied load is all transferred by the HE fibres at the cross section considered. The mathematical expression of the failure strain of this case is the same as Equation 8.

In the case of non-hybrid composite,

$$\epsilon_2 = [2NL\delta p^2(k^q - 1)]^{-1/2q} \quad (12)$$

is the lower bound of the failure strain.

As has been mentioned in the Introduction, the hybrid effect is the enhancement of the initial failure strain which corresponds to the failure of LE fibres. Therefore, Equation 7 should be compared with Equation 12 in order to discuss the hybrid effect. The hybrid effect may be calculated as

$$R_\epsilon = \left[\frac{\delta_h(k_h^q - 1)}{2\delta(k^q - 1)} \right]^{-1/2q} \quad (13)$$

from Equations 8 and 12. It is necessary to know the values δ , δ_h , k , k_h , and q to calculate R_ϵ . Other Weibull parameters, p , r , s , are not necessary.

If we want to know the enhancement of ultimate failure strain, p , r , and s also becomes necessary from Equation 10. The mean values of Weibull distributions of Equation 1 can be expressed as follows:

$$\begin{aligned} \bar{\epsilon}(l) &= (pl)^{-1/q} \Gamma(1 + 1/q) \\ \bar{\epsilon}^*(l) &= (rl)^{-1/s} \Gamma(1 + 1/s) \end{aligned} \quad (14)$$

where Γ is the gamma function. The Weibull parameters p and r can therefore be expressed by $\bar{\epsilon}$ and $\bar{\epsilon}^*$, although the expression is complicated. In a special case of $q = s$, the enhancement of final failure strain R^* ($= \epsilon_{2h}^*/\epsilon_2$) is easy to calculate and the result is

$$R_\epsilon^* = \left(\frac{2\delta}{\delta_h} \right)^{1/2q} \left(\frac{\bar{\epsilon}^* k}{\bar{\epsilon} k_h^*} \right)^{1/2} \quad (15)$$

where $k_h^q - 1 \simeq k_h^q$ and $k^q - 1 \simeq k^q$ are assumed. The failure strain enhancements can be calculated from Equations 13 and 15.

3. Numerical calculations and discussions

We consider here two combinations of materials:

graphite/glass [35] and Kevlar[®]/graphite [36] hybrids.

The first example is the experimental data of Bunsell and Harris [35] where high modulus graphite/E-glass laminated hybrids were tested. The ratio of extensional rigidities of two kinds of fibres is defined as

$$R = E^*A^*/EA \quad (16)$$

Young's moduli of graphite and glass composites were 142 and 41 GPa, respectively. Strictly speaking, Young's moduli of graphite and glass fibres themselves must be used in the calculation of Equation 16. But it may not have so much error even if we put $R = 41/142 = 0.289$, for the present case. The SCFs are calculated in the Appendix to be $k_h = 1.129$ and $k_h^* = 1.862$. The SCF in a non-hybrid composite is $k = 1.333$. The dimensionless ineffective length, $\delta/(EAd/GH)^{1/2}$ and $\delta_h/(EAd/Gh)^{1/2}$, are 1.571 and 1.713, respectively (see Appendix).

The representative value of Weibull parameter, q , is said to be 5 to 8 for single glass fibres or graphite fibres and 20 for a yarn or bundle of fibres. In this paper, $q = 20$ is adopted in accordance with Zweben [28], which approximately corresponds to 6% of coefficient of variation of the failure strain of fibres.

Substituting these values into Equation 13 we get $R_\epsilon = 1.11$. We have not accounted for the hybrid effect induced by the residual thermal strain which is about 10% of failure strain [35]. If we add this amount, the hybrid effect should be modified to $R_\epsilon = 1.21$. Since we considered 50:50 hybrids, this value must be compared with the experimental data of four-layer hybrids, $R_\epsilon(\text{exp}) = 1.31$ [35]. Our prediction is fairly close to the experimental value.

The enhancement of the ultimate failure strain can be calculated from Equation 15 as $R_\epsilon = 2.23$ where the experimental values of $\bar{\epsilon} = 0.26$ and $\bar{\epsilon}^* = 1.75$ were used. This value corresponds to Zweben's $R_\epsilon = 2.26$ where we must again point out that these are not for the enhancement of initial failure strain (hybrid effect) but for the enhancement of ultimate failure strain.

If all LE fibres are broken prior to the first failure of HE fibres, the SCF becomes, from Equation 11, $k_h^* = 1 + 1/0.289 = 4.46$. Then, from Equation 15, we get $R_\epsilon^* = 1.44$. This shows the failure of HE fibres occurs between $(1.44-2.23)\bar{\epsilon}$.

From these data we can draw the stress-strain

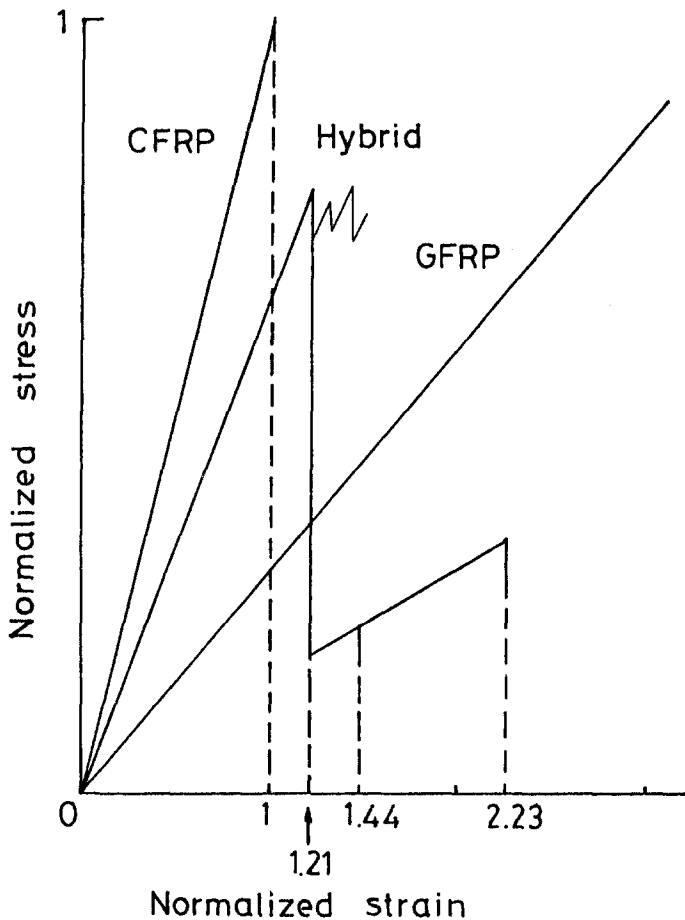


Figure 4 Predicted stress-strain behaviour of CFRP, GFRP and hybrid composites.

curve as shown in Fig. 4. This figure resembles the results by Bunsell and Harris [35]. That is, the initial failure strain is larger than that of the LE fibre composite and the ultimate failure strain is smaller than that of the HE fibre composite. Although the shape of the curve is fairly different from the experimental data where a saw-shape pattern appears, this can not be interpreted by our present model; some other model like the Monte Carlo simulation [29–31] is necessary in order to explain the experimental stress-strain curve in more detail.

Zweben [28] measured hybrid effects for Kevlar 49/graphite (Thornel 300). In this case, Young's moduli of graphite and Kevlar[®] were 34 and 19×10^6 psi, respectively, from Table I of [36]. R is calculated as $R = 0.56$. From the Appendix, $k_h = 1.074$, $k_h^* = 1.528$, and $\delta_h / (EAd/Gh)^{1/2} = 1.633$ are obtained. Again assuming $q = 20$, $R_e = 1.13$ is calculated from Equation 13. The experimental values were $R_e = 1.04$ for unidirectional hybrids and $R_e = 1.31$ for blanch

fabrics [28]. Our predicted value falls in between these two experimental values.

As for the ultimate failure strain $R_e^* = 1.24$ is the predicted value where $\bar{\epsilon} = 1.04$ and $\bar{\epsilon}^* = 1.80$ were used [28]. In the case that all LE fibres are broken, the SCF becomes, from Equation 11, $k_h^* = 2.78$ and Equation 14 reduces to $R^* = 0.916$. This value is peculiar because it is smaller than unity. We may conclude that if all LE fibres are broken, the failure of HE fibres will occur catastrophically in a case of Kevlar[®]/graphite hybrids.

In this paper, we used a criterion close to a diplet to evaluate the failure of hybrid composites. In a more precise manner, a 3-plet or 4-plet model should be used. This kind of problem is basically possible to solve because we have already solved a general solution of the SCF in r successive broken fibres in [38], although it may need some effort.

4. Conclusions

Although there are many excellent points in the study of Zweben [28], there are some unclear

points. We tried a modification of his theory in this paper. The meaning of initial failure (according to the hybrid effect) was made clear in the present statistical calculation. More precise SCFs than Zweben's approximate values were calculated by means of shear-lag analysis. By these modifications, tensile behaviour of hybrid composite has become to be predicted in more precise manner.

Acknowledgements

This work is partly supported by the Ministry of Education, Japan, under contract number 57350003.

Appendix: Stress concentration factors and ineffective length

Since we have already reported the analysis for the SCF of an intraply hybrid sheet [37, 38], an interply laminate [31], and an intraply laminate [39], only a brief summary of the procedure is shown here.

Fig. 2 shows a model of analysis where a tensile load is applied to the fibre direction. Applying the well known shear-lag assumptions [33, 40, 41], the equilibrium of force of the m -th fibres (LE and HE, respectively) are

$$EA \frac{d^2 u_m}{dx^2} + \frac{Gh}{d} (u_m^* + u_{m-1}^* - 2u_m) = 0 \quad (A1)$$

$$E^*A^* \frac{d^2 u_m^*}{dx^2} + \frac{Gh}{d} (u_{m+1} + u_m - 2u_m^*) = 0$$

where u_m is the displacement of the m -th fibre and EA and G denote, respectively, the fibre extensional stiffness and the shear modulus of the matrix. h and d are defined in Fig. 2.

The force-displacement relations are

$$p_m = EA \frac{du_m}{dx} \quad p_m^* = E^*A^* \frac{du_m^*}{dx} \quad (A2)$$

where p_m is the axial load of m -th fibre. The boundary conditions are

$$\begin{aligned} p_m(0) = 0 \quad (m = 0) \quad u_m(0) = 0 \quad (m \neq 0) \\ u_m^*(0) = 0 \quad p_m^*(\infty) = \frac{E^*A^*}{EA} p \quad (A3) \\ p_m(\infty) = p, \end{aligned}$$

By introducing the following dimensionless parameters

$$\begin{aligned} P_m = p_m/p \quad P_m^* = p_m^*/p \\ U_m = u_m/p(d/EAGh)^{1/2} \quad U_m^* = u_m^*/p(d/EAGh)^{1/2} \end{aligned}$$

$$\xi = x/(EAd/Gh)^{1/2} \quad R = E^*A^*/EA \quad (A4)$$

Equations A1 to A3 can be expressed as follows:

$$U_m'' + U_m^* + U_{m-1}^* - 2U_m = 0 \quad (A5)$$

$$RU_m'' + U_{m+1} + U_m - 2U_m^* = 0$$

$$P_m = U_m' \quad P_m^* = RP_m' \quad (A6)$$

$$P_m(0) = 0 \quad (m = 0) \quad U_m(0) = 0 \quad (m \neq 0)$$

$$U_m^*(0) = 0 \quad (A7)$$

$$P_m(\infty) = 1 \quad P_m^*(\infty) = R$$

where $()' = d()/d\xi$.

The following influence functions initially proposed by Hedgepeth [33] are applied here:

$$U_m(\xi) = \xi + V_m(\xi)U_0(0) \quad (A8)$$

$$U_m^*(\xi) = \xi + V_m^*(\xi)U_0(0)$$

where V and V^* are the influence functions. Thus Equations A5 and A7 reduce to

$$V_m'' - 2V_m + V_m^* + V_{m-1}^* = 0 \quad (A9)$$

$$RV_m'' - 2V_m^* + V_{m+1} + V_m = 0$$

$$V_m(0) = 1 \quad (m = 0) \quad V_m(0) = 0 \quad (m \neq 0)$$

$$V_m^*(0) = 0 \quad (A10)$$

$$V_m'(\infty) = 0 \quad V_m^*(\infty) = 0$$

To solve Equations A9 the following Fourier series expressions are introduced

$$\bar{V} = \sum_{m=-\infty}^{\infty} V_m \exp(-im\theta) \quad (A11)$$

$$\bar{V}^* = \sum_{m=-\infty}^{\infty} V_m^* \exp(-im\theta)$$

or inversely,

$$V_m = \frac{1}{2\pi} \int_{-\pi}^{\pi} \bar{V} \exp(im\theta) d\theta \quad (A12)$$

$$\bar{V}_m^* = \frac{1}{2\pi} \int_{-\pi}^{\pi} \bar{V}^* \exp(im\theta) d\theta$$

Then, multiplying Equations 9 by $\exp(-im\theta)$ and summing over all m give

$$\bar{V}'' - 2\bar{V} + [1 + \exp(-i\theta)] \bar{V}^* = 0 \quad (A13)$$

$$R\bar{V}^* - 2\bar{V}^* + [1 + \exp(i\theta)] \bar{V} = 0$$

Equations A10 can also be expressed by \bar{V} and \bar{V}^* , although the detail is not shown here.

The solutions of Equations A13 are

$$\bar{V} = C_1 \exp(-\lambda_1 \xi) + C_2 \exp(-\lambda_2 \xi) \quad (\text{A14})$$

$$\bar{V}^* = C_3 \exp(-\lambda_1 \xi) + C_4 \exp(-\lambda_2 \xi)$$

where

$$\lambda_1 = [a + (a^2 - b)^{1/2}]^{1/2}$$

$$\lambda_2 = [a - (a^2 - b)^{1/2}]^{1/2}$$

$$a = 1 + 1/R \quad b = 2(1 - \cos \theta)/R$$

$$C_1 = (2 - \lambda_2^2)\Lambda \quad C_2 = -(2 - \lambda_1^2)\Lambda$$

$$C_3 = (2 - \lambda_1^2)(2 - \lambda_2^2)\Lambda/[1 + \exp(-i\theta)]$$

$$C_4 = -C_3 \quad \Lambda = 1/(\lambda_1^2 - \lambda_2^2) \quad (\text{A15})$$

The SCF of the adjacent HE fibre (k_h^*) and next-adjacent LE fibre (k_h) are, from the definition,

$$k_h^* = P_0^*(0)/P_0^*(\infty) = 1 + V_0^*(0)'U_0(0) \quad (\text{A16})$$

$$k_h = P_1(0)/P_1(\infty) = 1 + V_1(0)'U_0(0)$$

where $U_0(0)$ can be calculated from the first condition of Equations A7.

Next we will calculate the ineffective length, δ_h . There are two ways of defining the ineffective length. Rosen [12] defined it as the length from the fibre end to the point where the axial load of the fibre recovers to ϕ ($=0.9$ to 0.95) of the load remote from the broken end. Another is defined as [28]

$$\frac{\delta_h}{2} = \int_0^\infty \left(\epsilon - \frac{du_0}{dx} \right) dx \quad (\text{A17})$$

which has been defined by replacing the actual

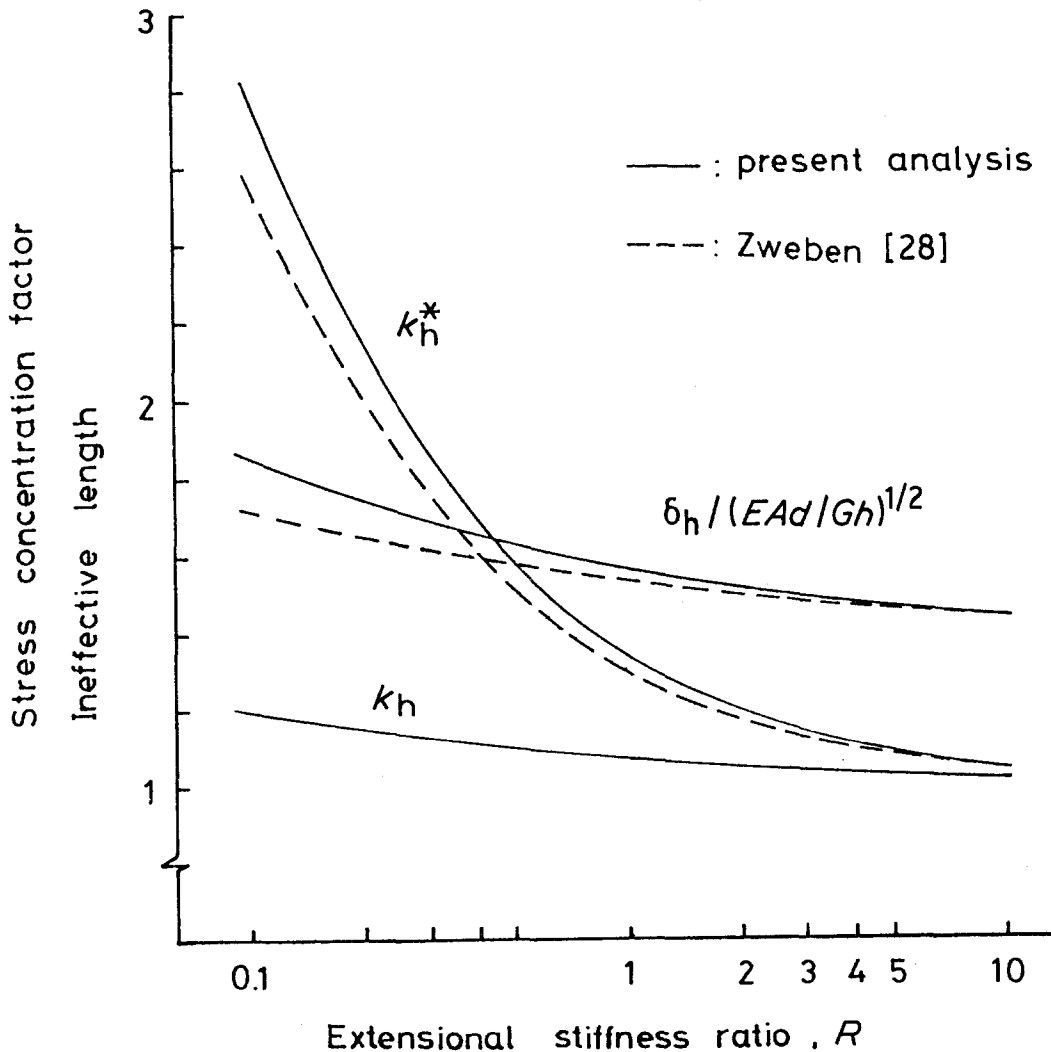


Figure A1 Stress concentration factor and ineffective length against extensional stiffness ratio, R .

fibre stress (or strain) distribution with equivalent step function. We follow the latter definition.

Substituting necessary equations into Equation A17, we get finally

$$\begin{aligned}\delta_h &= 2(EAd/Gh)^{1/2}U_0(0)\int_0^\infty\left(-\frac{dV_0}{d\xi}\right)d\xi \\ &= 2(EAd/Gh)^{1/2}U_0(0)\end{aligned}\quad (\text{A18})$$

The following expression may be convenient:

$$\delta_h/(EAd/Gh)^{1/2} = 2U_0(0) \quad (\text{A19})$$

In the case of ordinary composite ($R = 1$), $U_0(0)$ was calculated as $\pi/4$ [37]. Thus the dimensionless ineffective length becomes $\pi/2$ which is a little larger than Zweben's result, 1.531 (cf. Equation A26 of [28]).

Fig. A1 depicts the SCF and ineffective length against extensional stiffness ratio of fibres (R). With decreasing R , both k_h and k_h^* increase. This is reasonable because the effect of broken LE fibre is large at small R , from the definition of R , Equation 16. The SCF of the next-adjacent LE fibre, k_h , is relatively small and this is advantageous for hybrid composites. At $R = 0.289$, which corresponds to high modulus graphite/glass hybrids, the SCF becomes $k_h = 1.129$ and $k_h^* = 1.862$ and $\delta_h/(EAd/Gh)^{1/2}$ is 1.713. In the case of $R = 0.56$, $k_h = 1.074$, $k_h^* = 1.528$, and $\delta_h/(EAd/Gh)^{1/2} = 1.633$ are obtained.

Zweben's approximate solutions are also shown in Fig. A1 by broken lines. His results predicts a little smaller SCF and ineffective length.

References

- J. R. VINSON, On the State of Technology and Trends in Composite Materials in the United States, in "Composite Materials: Mechanics, Mechanical Properties and Fabrication", edited by K. Kawata and T. Akasaka (Japan Society for Composite Materials, Tokyo, 1981) p. 353.
- T. HAYASHI, *Fukugo Zairyo (Compos. Mater.)* 1 (1972) 18.
- T. HAYASHI, K. KOYAMA, A. YAMAZAKI and M. KIHARA, *Fukugo Zairyo (Compos. Mater.)* 1 (1972) 21.
- K. R. BERG, 27th Annual Technical Conference of SPI (1972) 17E.
- T. FUJII and K. TANAKA, *Zairyo* 21 (1972) 906 (in Japanese).
- I. L. KALNIN, ASTM STP 497 (American Society for Testing and Materials, Philadelphia, 1972) p. 551.
- T. W. CHOU and A. KELLY, *Ann. Rev. Mater. Sci.* 10 (1980) 229.
- W. J. RENTON, An Overview of Hybrid Composite Applications to Advanced Structures, in "Composite Materials: Mechanics, Mechanical Properties and Fabrication", edited by K. Kawata and T. Akasaka (Japan Society for Composite Materials, 1981) p. 362.
- H. FUKUDA, *J. Jpn. Soc. Compos. Mater.* (in Japanese) to be published.
- P. W. MANDERS and M. G. BADER, *J. Mater. Sci.* 16 (1981) 2233.
- Idem, ibid.* 16 (1981) 2246.
- B. W. ROSEN, *AIAA J.* 2 (1964) 1985.
- C. ZWEBEN, *ibid.* 6 (1968) 2325.
- H. FUKUDA and K. KAWATA, *Trans. Jpn. Soc. Compos. Mater.* 2 (1976) 59.
- I. KIMPARA, I. WATANABE, T. OHKATSU and N. UEDA, "A Simulation of Failure Process of Fibre-Reinforced Materials," 7th Symposium on Composite Materials, JUSE, Japan, (1974) p. 169 (in Japanese).
- H. FUKUDA and K. KAWATA, *Fibre Sci. Technol.* 10 (1977) 53.
- O. OKUNO and I. MIURA, *J. Jpn. Soc. Met.* 42 (1978) 736 (in Japanese).
- K. P. OH, *J. Compos. Mater.* 13 (1979) 311.
- D. G. HARLOW and S. L. PHOENIX, *ibid.* 12 (1978) 195.
- D. G. HARLOW and S. L. PHOENIX, *ibid.* 12 (1978) 314.
- R. E. PITT and S. L. PHOENIX, *Textile Research J.* 51 (1981) 408.
- V. V. BOLOTIN, *Eng. Fract. Mech.* 8 (1976) 103.
- V. V. BOLOTIN, "Stochastic Models of Fracture of Unidirectional Fibre Composites," 2nd US-USSR Conference on Composite Materials (1980) p. 3.
- B. BERGMAN, *J. Compos. Mater.* 15 (1981) 92.
- S. B. BATDORF, *J. Reinforced Plast. Comp.* 1 (1982) 153.
- Idem, ibid.* 1 (1982) 165.
- H. SUEMASU, *Trans. Jpn. Soc. Compos. Mater.* in press.
- C. ZWEBEN, *J. Mater. Sci.* 12 (1977) 1325.
- T. W. CHOU and H. FUKUDA, Stiffness and Strength of Hybrid Composites, in "Composite Materials: Mechanics, Mechanical Properties and Fabrication", edited by K. Kawata and T. Akasaka (Japan Society for Composite Materials, 1981) p. 78.
- H. FUKUDA and T. W. CHOU, *J. Compos. Mater.* 16 (1982) 371.
- H. FUKUDA and K. KAWATA, *Trans. Jpn. Soc. Aero. Space Sci.* 25 (1983) 203.
- C. ZWEBEN, *Eng. Fract. Mech.* 6 (1974) 1.
- J. M. HEDGEPEETH, "Stress Concentrations in Filamentary Structures," NASA TN D-882 (1961).
- C. ZWEBEN and B. W. ROSEN, *J. Mech. Phys. Solids* 18 (1970) 189.
- A. R. BUNSELL and B. HARRIS, *Composites* 5 (1974) 157.
- C. ZWEBEN, Proceedings of the 1975 International Conference on Composite Materials (ICCM, 1975) p. 345.
- H. FUKUDA and T. W. CHOU, *Trans. Jpn. Soc. Compos. Mater.* 7 (1981) 37.

38. H. FUKUDA and T. W. CHOU, "Stress Concentrations in a Hybrid Composite Sheet," *J. Appl. Mech.* in press.
39. H. FUKUDA and K. KAWATA, "Comparison of Interply and Intraply Hybrid Composites from a View Point of Stress Concentration," submitted for publication.
40. J. M. HEDGEPEETH and P. VAN DYKE, *J. Compos. Mater.* **1** (1967) 294.
41. X. JI, G. C. HSIAO and T. W. CHOU, *ibid.* **15** (1981) 443.

*Received 18 April
and accepted 21 July 1983*